Edith Cowan University

Research Online

Research outputs 2022 to 2026

6-1-2023

Performance enhancement of photovoltaic-thermal modules using a new environmentally friendly paraffin wax and red wine-rGO/H2O nanofluid

Hossein Nabi

Mosayeb Gholinia

Mehdi Khiadani
Edith Cowan University

Abdellah Shafieian
Edith Cowan University

Follow this and additional works at: https://ro.ecu.edu.au/ecuworks2022-2026

 Part of the Chemical Engineering Commons

10.3390/en16114332
Nabi, H., Gholinia, M., Khiadani, M., & Shafieian, A. (2023). Performance enhancement of photovoltaic-thermal modules using a new environmentally friendly paraffin wax and red wine-rGO/H2O nanofluid. Energies, 16(11), 4332. https://doi.org/10.3390/en16114332
This Journal Article is posted at Research Online.
https://ro.ecu.edu.au/ecuworks2022-2026/2569

energies

MDPI

Article

Performance Enhancement of Photovoltaic-Thermal Modules Using a New Environmentally Friendly Paraffin Wax and Red Wine-rGO/H_2O Nanofluid

Hossein Nabi [1], Mosayeb Gholinia [2], Mehdi Khiadani [3] and Abdellah Shafieian [3,*]

[1] Department of Mechanical Engineering, Mazandaran University of Science and Technology, Babol 47166-85635, Iran
[2] Department of Mechanical Engineering, Babol Noushirvani University of Technology, Babol 47148-71167, Iran
[3] School of Engineering, Edith Cowan University, 270 Joondalup Drive, Joondalup, Perth, WA 6027, Australia; m.khiadani@ecu.edu.au
* Correspondence: a.shafieiandastjerdi@ecu.edu.au; Tel.: +61-8-6304-6548

Abstract: Photovoltaic/thermal systems are one of the most efficient types of solar collectors because they absorb solar radiation and generate electricity and heat simultaneously. For the first time, this paper presents an investigation into the impact of red wine-rGO/H_2O nanofluid and paraffin wax on the thermohydraulic properties of a photovoltaic/thermal system. The study focuses on three innovative nonlinear arrangements of the serpentine tubes. The effects of these materials and configurations are analyzed through numerical simulations. To improve the performance, environmentally friendly materials, including red wine-rGO/H_2O nanofluid and paraffin wax, have been used. Various performative parameters such as electrical and thermal efficiency of the photovoltaic/thermal system, exergy, and nanofluid concentration were investigated. The results demonstrated a significant enhancement in the system's performance when using innovative serpentine tubes instead of simple tubes for the fluid flow path. The use of paraffin C18 increases electrical efficiency, while the use of paraffin C22 improves thermal efficiency. Moreover, the incorporation of phase change materials along with the utilization of innovative geometries in the serpentine tube led to a notable improvement in the outlet temperature of the fluid, increasing it by 2.43 K. Simultaneously, it substantially reduced the temperature of the photovoltaic cells, lowering it by 21.55 K. In addition, the new model demonstrated significant improvements in both thermal and electrical efficiency compared to the simple model. Specifically, the maximum thermal efficiency improvement reached 69.2%, while the maximum electrical efficiency improvement reached 11.7%.

Keywords: photovoltaic/thermal (PV/T) systems; eco-friendly nanofluid; thermal efficiency; electrical efficiency; PCM:C18; PCM:C22

check for updates

Citation: Nabi, H.; Gholinia, M.; Khiadani, M.; Shafieian, A. Performance Enhancement of Photovoltaic-Thermal Modules Using a New Environmentally Friendly Paraffin Wax and Red Wine-rGO/H_2O Nanofluid. *Energies* **2023**, *16*, 4332. https://doi.org/10.3390/en16114332

Academic Editor: Carlo Renno

Received: 22 March 2023
Revised: 15 May 2023
Accepted: 15 May 2023
Published: 25 May 2023

Copyright: © 2023 by the authors. Licensee MDPI, Basel, Switzerland. This article is an open access article distributed under the terms and conditions of the Creative Commons Attribution (CC BY) license (https://creativecommons.org/licenses/by/4.0/).

1. Introduction

The need for energy is considered one of the most important human needs. Fossil fuels have been the most important source of energy supply for many years. One of the biggest problems with these fuels is their pollution and limitations. For this reason, numerous countries currently striving to develop the necessary equipment to harness renewable energy as a clean and permanent source of energy [1,2]. One of the most important renewable energies is solar energy, which is converted into usable electrical energy through the utilization of solar panels. The analysis of energy and exergy parameters of solar panels serves as an initial step in the advancement of this technology, establishing an appropriate standard for measuring the performance of solar panels [3,4]. Energy analysis is based on the first law of thermodynamics, and exergy analysis is based on the second law of thermodynamics. While photovoltaic cells are primarily used to produce electrical energy, they can also be used for a wide range of applications, including thermal applications

such as solar water heaters [5,6]. In addition, photovoltaic–thermal systems (PV/Ts) have also developed a lot in recent years, which perform the two mentioned functions at the same time. Researchers have conducted numerous experimental and numerical studies to enhance the efficiency of these collectors [7,8]. Due to the importance of energy and exergy analysis in PV/T systems, many researchers have focused on this topic.

In a research paper on hybrid collectors, Dupeyrat et al. [9] investigated the thermal and electrical performance of a PV/T system. The results of this article show the better performance of PV/T compared to PV in the limited space of a building. Alous et al. [10] conducted an experimental study to evaluate the impact of adding a thermal unit to a photovoltaic module. They concluded that the use of a thermal unit increases the total energetic efficiency by 53.4% for distilled water. In another study, Sotehi et al. [11] proposed a hybrid photovoltaic–thermal system for freshwater production, considering net-zero energy buildings. The results of this article showed an increase of 2.97 times in the annual production of freshwater compared to passive solar stills. Additionally, in the article published by Nasrin et al. [12], the effect of fluid flow rate and cooling on the electrical and thermal efficiency of a PV/T system was analyzed. The findings indicated that the additional cooling resulted in a 7% reduction in output power. In a very similar work, Nižetić et al. [13] reported this reduction in output power to be between 0.25% and 0.5%. Idoko et al. [14] used an aluminum heat sink connected to the back of the photovoltaic system to reduce the maximum temperature of the module surface. This creative mechanism was able to increase the thermal efficiency of the photovoltaic system by about 3%.

Based on the above literature, significant progress has been achieved in the field of solar energy conversion systems. These advancements offer promising solutions to address common challenges encountered in PV/T systems. Further investigating some passive methods, such as the use of nanofluids, changing the shape of the tube, and phase-change materials, holds the potential to address the aforementioned challenges effectively. One of the techniques that can be used to achieve higher electrical–thermal efficiency is the use of phase change materials (PCM) [15,16]. The phase change materials are latent heat storage materials that can have a higher thermal energy storage density compared to sensible heat storage materials. They can absorb or release a large amount of energy at a constant temperature even after thousands of cycles of the phase change process. The phase change materials used in the design of PV/T systems must have the following characteristics [17,18]:

- Thermal properties: proper phase change temperature, high latent heat of phase change, good heat transfer.
- Physical properties: favorable phase balance, high density, low volume change, low vapor pressure, renewable phase change.
- Economic properties: availability, reasonable price, recyclability.

The use of nanoparticles in the base fluid is another effective solution to increase the energy storage of PV/T systems. Among these nanoparticles, graphene, in which the ballistic transfer of heat carriers occurs, has attracted more attention. Recently, the scientific community has shown a growing interest in synthesizing these nanoparticles using different plant extracts. This approach aims to broaden the range of applications for these nanoparticles while simultaneously reducing their environmental risks [19,20]. Due to the importance of analyzing PCM and environmentally friendly nanofluids, limited research has been conducted on this topic.

Sardarabadi et al. [21] analyzed the performance of a photovoltaic (PV) system using phase change materials and ZnO/water nanofluid in a laboratory study. The results of this paper show a 13% increase in electrical output in the presence of PCM. Nada et al. [22] investigated the use of nanofluid and PCM in a PV and concluded that the use of pure PCM and PCM together with Al_2O_3–H_2O nanofluid reduces the system temperature by 8.1 °C and 10.1 °C, respectively. Ghadikolaei et al. [23] investigated the thermal energy storage on the heat sink with two ideas: environmentally friendly nanofluids (CGNPs/H_2O) and

nature-based designs. Additionally, in a similar article, Ghadikolaei et al. [24] achieved a 6.83% increase in the thermal efficiency of a heat sink using environmentally friendly nanofluid (green graphene/H_2O). Cui et al. [25] evaluated the economic, environmental, and energy performance of a thermal photovoltaic (PV/T) system using PCM composites. The thermal efficiency of PV/T systems can increase by 20 to 30% with composite PCM.

The above literature in the field of PV/T cooling shows that the use of PCMs and environmentally friendly nanofluids is likely to improve the thermal performance of PV/T. In this CFD study, for the first time, the application of PCM and an environmentally friendly nanofluid (red wine-rGO/H_2O) to improve the thermal energy storage in a PV/T is investigated. It should be acknowledged that despite much research in this field, no study has examined PCMs with red wine-rGO/H_2O nanofluid in different concentrations with these nonlinear flow paths. Therefore, the objectives of this environmental paper include (a) achieving an optimal design of the cooling path in a PV/T, (b) analyzing two PCM models in electrical-thermal efficiency, (c) evaluating the effect of red wine-rGO/H_2O nanofluid concentration in the thermal energy storage process, and (d) putting together the results of the simultaneous use of an eco-friendly nanoparticle, PCM, and different flow path designs.

2. Materials and Methods

This article aims to investigate the electrical–thermal performance of a PV/T with three different geometries of the fluid flow path in the presence of eco-friendly nanofluid and phase change materials (see Figure 1). The proposed geometry components, including glass, ethyl vinyl acetate (EVA), photovoltaic (PV) cells, EVA, Tedlar, absorber tubes, phase change material (PCM), and insulation, are arranged in a 3D physical model using CATIA-V5 software (see Figure A1 in Appendix A). The heat transfer fluid in this article is red wine-rGO/H_2O, which is an appropriate example to expand research in the chemical-mechanical field in order to increase the efficiency of PV/T collectors. These nanoparticles in four different concentrations (ϕ = 1% to 4%) have been simulated. The model utilized in this study is a 40 W monocrystalline silicon photovoltaic (PV) module manufactured by Suntech (China) and designed using CATIA 2019 software.

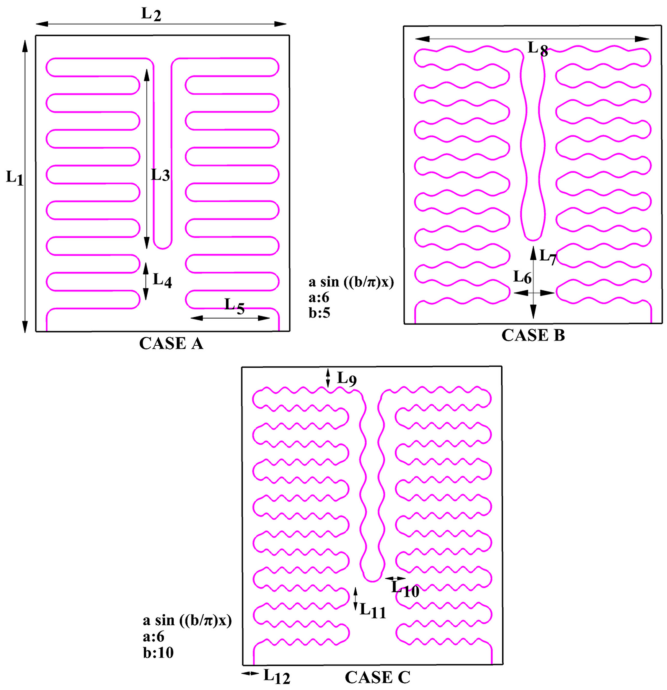

Figure 1. Geometries of nonlinear serpentine tubes. L1: 630 mm, L2: 540 mm, L3: 367 mm, L4: 76 mm, L5: 160 mm, L6: 100 mm, L7: 180 mm, L8: 456 mm, L9: 43 mm, L10: 22 mm, L11: 38 mm.

According to Figure A1, the length and width of the PV/T system are 540 and 630 mm, respectively, and the area where the nanofluid tubes are located is 587 × 456 mm [26]. Additionally, the material of the absorbent tubes is selected from copper because the stability of copper against factors such as boiling and high voltage environments is relatively good. Some important thermo–physical properties of different PV/T components are reported in Table A1. The general perspective of this simulation is as follows:

- Analysis of three new non-linear arrangements $(a \times sin\ ((b\pi)x))$ of the absorber tube for more fluid circulation and creating a higher temperature gradient between the structure and the fluid. In this non-linear equation, parameters a and b are variables.
- In the analysis of the electrical and thermal efficiency of the proposed designs with two types of phase change materials (PCM:Paraffin C18 and PCM:Paraffin C22), the simulated paraffin wax volume is about 2 kg.
- Analysis of fluid outlet temperature, PV/T-PCM surface temperature, and electrical and thermal efficiency in the presence of an eco-friendly nanofluid (red wine-rGO/H_2O) for different concentrations (ϕ = 1% to 4%).

2.1. Boundary Conditions and Initial Conditions

CFD simulation is performed using ANSYS-Fluent 18.2 software under the turbulent flow regime and with a single-phase model. In this simulation, solar radiation enters the PV/T-PCM surface with a uniform heat flux (1000 W/m^2) from the upper (vertical) wall. Seven U-shaped copper rings are located in two rows on the surface of the PV/T-PCM system. These rings facilitate convective heat transfer between the red wine-rGO/H_2O nanofluid and the system, as well as conductive heat transfer with walls. The eco-friendly nanofluid enters the system at an inlet temperature of 303.15 K. It follows a constant mass flow rate of 30 kg/h and exits from the copper pipe with a pressure outlet condition where the relative pressure is zero. The ambient temperature is 35 °C, the melting temperature of PCM is in the range of 302 K–317 K, and the wind speed is assumed to be 1 m/s. According to the first law of thermodynamics, the total input energy to PV/T-PCM is equal to the solar radiation received, which is 340.2 W. The output energies from the system include convective losses (58 W), electrical energy (45 W), radiation losses (93 W), and useful heat (143 W). The error in these calculations is 0.35%, and the difference between the total input and output energy is 1.2 W. The assumption of non-slip and adiabatic boundary conditions for all outer walls in this simulation is established. Eco-friendly, incompressible, and Newtonian nanofluid (red wine-rGO/H_2O) in four different concentrations of nanoparticles (ϕ = 1% to 4%) is entered into the software by writing C++ code. Additionally, in this simulation, the model is solved transiently, which means that time changes are considered. The thickness of the adhesive layer between the absorber and the panel, gravity, and natural convection through the PCM were ignored.

2.2. Governing Equations

The 3D simulation f the system was performed using ANSYS-Fluent software, utilizing the finite volume method (FVM). The software solved the Newtonian, stable, and viscous incompressible fluid flow by employing the Navier–Stokes equations. Additionally, the temperature distribution was solved using the thermal energy equation. In general, continuity, momentum, and energy equations are applied according to research [26].

The governing equations for the above literature are as follows:

$$\text{Continuity}: \quad \frac{\partial \rho}{\partial t} + \nabla \cdot \left(\rho \vec{V} \right) \tag{1}$$

$$\text{Momentum}: \quad \frac{\partial \rho V}{\partial t} + \nabla \cdot \left(\rho \vec{V} \vec{V} \right) = -\nabla P + \nabla \left(\mu \nabla \vec{V} \right) + \rho g + S \tag{2}$$

$$\text{Energy}: \quad \frac{\partial(\rho h)}{\partial t} + \nabla\cdot\left(\rho \vec{V} h\right) = \nabla\cdot(k\nabla T) \tag{3}$$

where P and V are pressure and velocity vectors, respectively.

The phase change materials in this article include paraffin waxes (PCM:Paraffin C18 and PCM:Paraffin C22) with a direct chain of n alkane CH_3-(CH_2)-CH_3. Chain crystals (CH_3) release a large amount of latent heat. Paraffin is resistant, safe, low-priced, and non-corrosive. To model the phase change process in PV/T-PCM, the porous enthalpy method is used. In this method, when the PCM is completely melted, the liquid fraction will be one, and when this material is completely solid, the liquid fraction will be zero. In the above equation, the liquid and solid interfaces are defined by the porous parameter S for the momentum equation [27,28]:

$$S = \left(\frac{1-\beta^2}{\beta^2+\varepsilon}\right)C\vec{V} \tag{4}$$

where C is a constant reflection of the mushy zone morphology, which is a region in which the liquid fraction β lies between zero and one. This constant is varied between 10^4 and 10^7, and thus 10^5 is considered for this paper. Parameter ε is a numerical value and is considered to be 0.001 to prevent division by zero.

$$\beta = \begin{cases} 0 & if \;\; T < T_s \\ 1 & if \;\; T > T_l \\ \frac{T-T_s}{T_l-T_s} & if \;\; T_s < T < T_l \end{cases} \tag{5}$$

In Equations (6) and (7), h is total enthalpy, which is the sum of latent enthalpy (h_{le}) and sensible enthalpy (h_{se}).

$$h_{se} = h_{\text{ref}} + \int_T^T C_p dT \tag{6}$$

$$h_{le} = \beta L \tag{7}$$

where h_{ref} is the reference enthalpy at temperature ($T_{ref} = 298.15$). To analyze the thermal and electrical efficiency of the system, these equations are used [29–31]:

$$\text{Electrical efficiency}: \quad \eta_{el} = \frac{\dot{E}_{el}}{\dot{E}_{sun}} = \eta_r\cdot[1 - 0.0045\cdot(T_{cell} - 298.15)] \tag{8}$$

where T_{cell} is the PV cell temperature and η_r is the PV module temperature at the standard condition.

$$\text{Thermal efficiency}: \quad \eta_{th} = \frac{\dot{E}_{el}}{\dot{E}_{sun}} = \frac{\dot{m}_{nf}\cdot C_{p,nf}\cdot\left(T_{nf,out} - T_{nf,in}\right)}{\dot{G}\cdot A_c\cdot\tau_c\cdot\alpha_{cell}} \tag{9}$$

The other constant values in Equations (8) and (9) can be seen in references [29,30]. Moreover, the thermal exergy of the present model can be presented as follows:

$$\text{Thermal exergy}: \dot{E}_{x,\;\; thermal} = \dot{m}C_{p\;fluid}\left[(T_{out}) - (T_{in}) - T_0 ln\frac{T_{out}}{T_{in}}\right] \tag{10}$$

It is worth noting that the pressure–velocity relationship was conducted with the conventional phase-coupled SIMPLE (PC-SIMPLE) method. The SIMPLE method solves the pressure equation implicitly and the velocity equation explicitly. Additionally, the momentum equations in the convective term are interpolated as a first-order upwind

scheme and energy as a second-order upwind scheme. The gradient in each cell is analyzed as a least-squares cell-based gradient. The under-relaxation factors for speed, energy, and pressure parameters are set to 0.9, 0.95, and 0.35, respectively. To reach an acceptable solution, the convergence criterion in the current CFD work is 10^{-8} for all variables.

2.3. Eco-Friendly Nanofluid Specifications

Research shows that the traditional synthesis of nanoparticles causes allergic skin reactions, environmental hazards, and aquatic mortality. Therefore, researchers related to the synthesis of nanoparticles are looking to reduce the above risks by using different plant extracts [32]. One of the great research projects in this field is the article by Sadri et al. [33,34] on the synthesis of graphene nanoparticles using red wine. Medical articles report that red wine has antimicrobial, anti-mutagenic, anti-cancer, and antioxidant activities [35]. The assumptions in the present 3D simulation for the environmentally friendly nanofluid (red wine-rGO/H_2O) are listed in Table A2 and Figure 2.

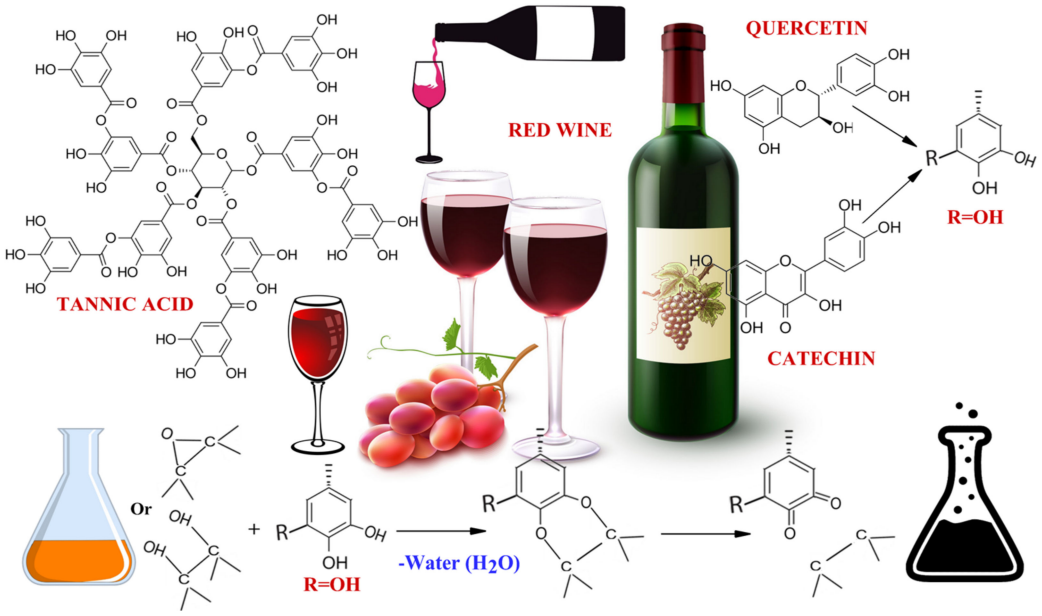

Figure 2. Schematic of the chemical components of the eco-friendly nanofluid.

2.4. Mesh Independence Study and Validation

Solving the CFD problem should be such that the changes in the results due to the mesh size can be ignored. Moreover, the meshing should be such that it has the highest density of cells near the solid walls (see Figure 3). The output data from the referenced article [26] regarding PV cell temperature reports that by changing the meshes from 4,000,000 to 11,000,000 for the simple model without the presence of PCM, the most optimal number of meshes is 94,000,000, which has a calculation error of less than 3%. The time step for all simulations is assumed to be 1 s, which was determined based on the comparison with the reference [26] for the simple model and PCM (C22), resulting in an error of less than 1%. The outputs related to grid independence and time step are shown in Figure 4. To validate the numerical model, the average temperature of the photovoltaic module and the electrical efficiency for three different models have been compared with the results from the experimental paper of Shahsavar et al. [36]. The comparison is presented in Figure 5. The maximum error rate for average PV temperature is about 0.17%, and the maximum error rate for electrical efficiency is about 0.72%.

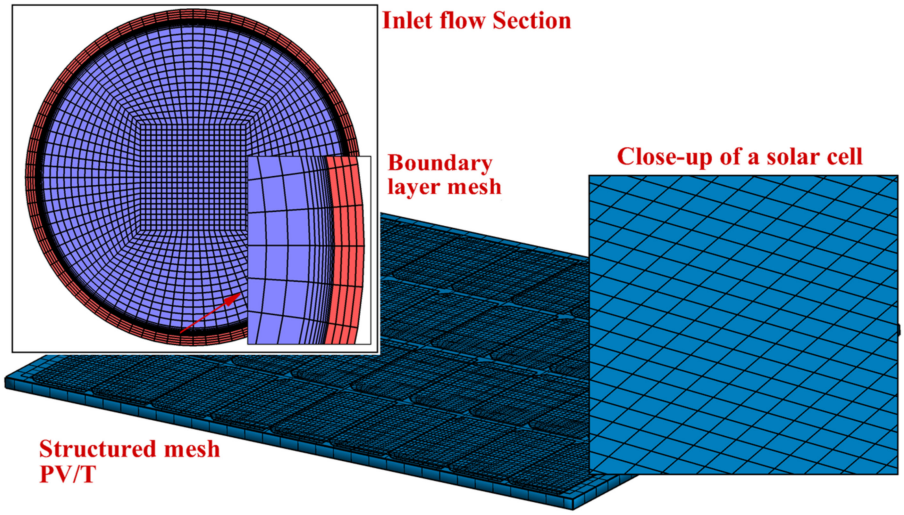

Figure 3. Mesh elements of the PVT system.

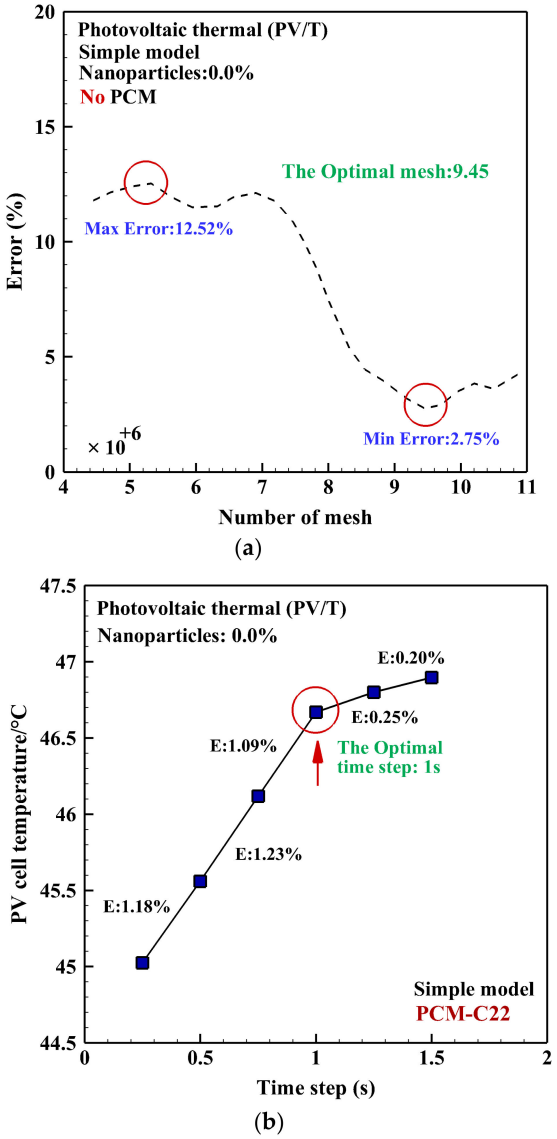

Figure 4. (**a**) Mesh independence and (**b**) time-step studies.

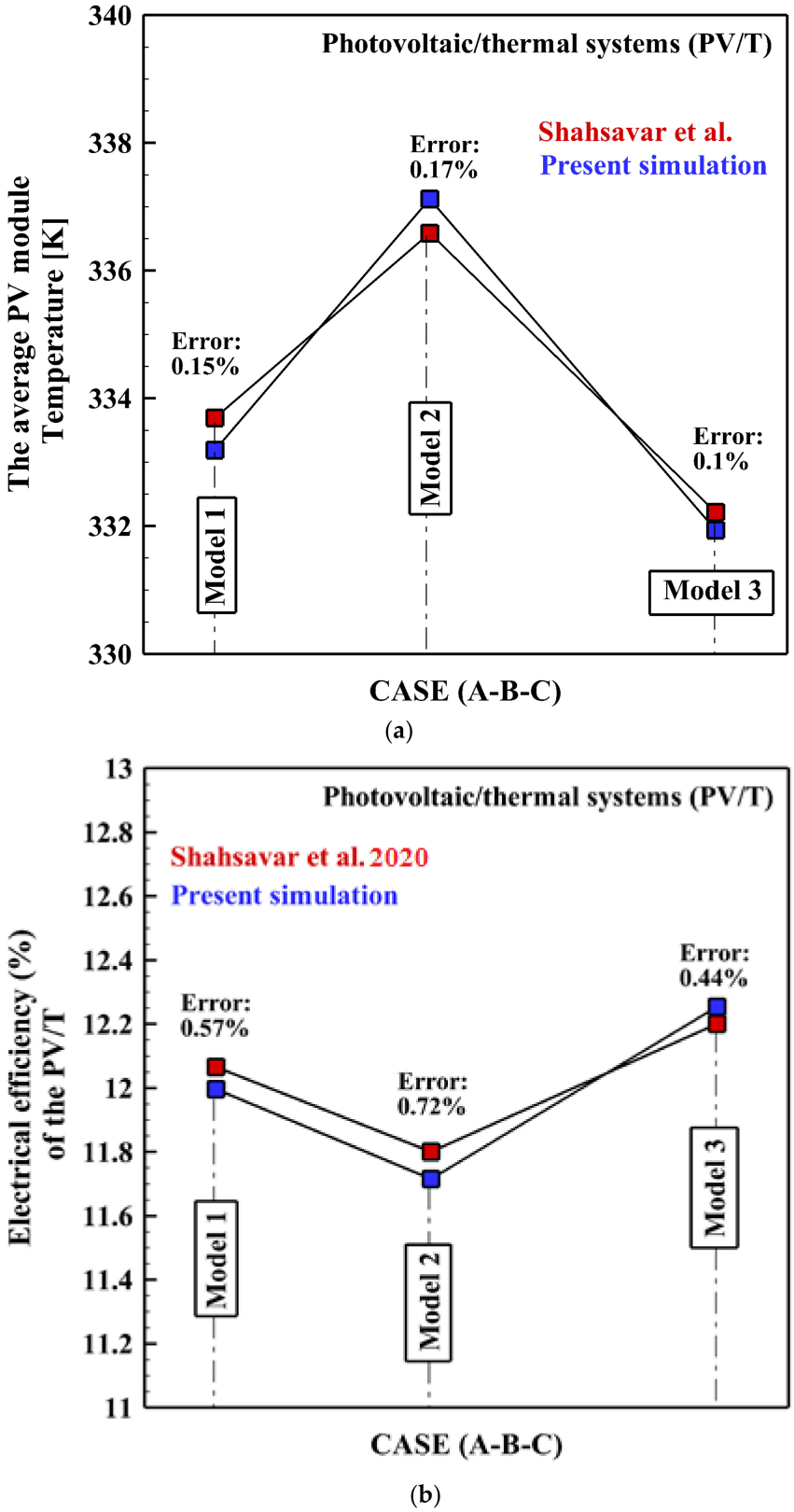

Figure 5. The numerical and experimental (**a**) average temperature and (**b**) electrical efficiency for PVT systems [36].

3. Results and Discussions

In this paper, innovative serpentine tubes, eco-friendly nanofluids, and PCMs are numerically examined to determine the best model for achieving the highest efficiency. As

it is known, the main objectives of PV/T simulations are to reduce the PV cell temperature and increase the output fluid temperature. In the first section, the PV cell temperature and the output fluid temperature were analyzed for two PCM materials. Once the optimal PCM material is determined, the subsequent section will investigate the effect of red wine-rGO/H_2O nanofluid concentration. In the second part, the thermal and electrical efficiencies in the presence of PCMs and different concentrations of green nanofluid will be examined.

3.1. PV/T Surface Temperature and Fluid Outlet Temperature

One of the parameters that must be evaluated in the design of PV/T systems is PV cell temperature. This parameter is more important for areas with a very hot climate because a sharp increase in temperature both reduces efficiency and causes thermal degradation. To investigate the effect of PCM on PV cell temperature, two different PCM models, including PCM:Paraffin C18 and PCM:Paraffin C22, were used in three innovative geometries (CASE A–C). A comparison was made with the case where no PCM was present, and the results are presented in Figure 6. As can be seen from Figure 6, the use of paraffin waxes has been able to significantly reduce the PV cell temperature and reduce the many disadvantages caused by the high temperature of the cell surface. According to Figure 6, the introduction of PCM:Paraffin C18 and PCM:Paraffin C22 in the PV/T system, without the presence of nanofluid, resulted in a decrease in PV cell temperature of approximately 4.30% and 1.84%, respectively, compared to the case without PCM. The reason for the reduction in the module surface temperature in the case of using the phase change material is the absorption of excess heat from the PV/T surface by the PCM. The comparison between PCM:C18 and PCM:C22 also shows the superiority of PCM:C18 in reducing PV cell temperature compared to PCM:C22. Physically, in order to achieve better efficiency, the melting point of PCMs should be in the working temperature range. This allows for the utilization of both sensible and latent thermal energy storage models simultaneously. Therefore, adding PCM:C22 to PV/T according to Table A3 is not beneficial for cooling the system due to its higher melting point.

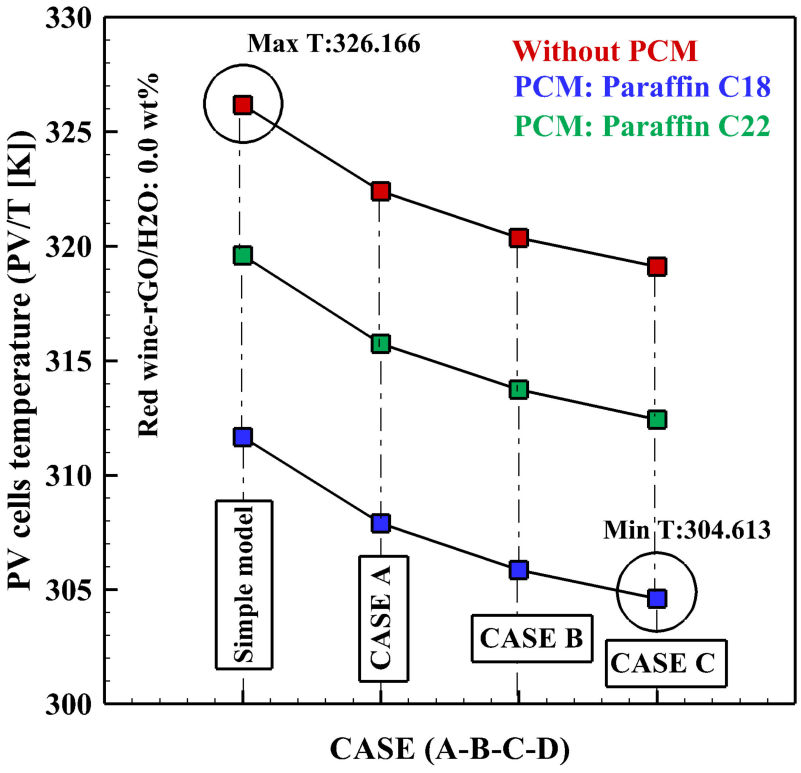

Figure 6. PV cell temperature in different models with and without PCMs.

Another parameter that should be evaluated in the design of PV/T systems is fluid outlet temperature because it directly affects thermal efficiency (see Figure 7). Based on Figure 7, when comparing simulations without PCM to simulations with PCM:C18 and PCM:C22 in a PV/T system using a simple model and without the presence of nanofluid, the fluid outlet temperature increased by approximately 0.22% and 0.55%, respectively. The reason for the increase in the output fluid temperature in the case of PCMs is the release of excess heat from the PV/T surface to the copper tube. The comparison between PCM:C18 and PCM:C22 also shows the superiority of PCM:C22 in increasing fluid outlet temperature compared to PCM:C18. In fact, after the PV heats up and reaches its maximum temperature, the PCMs in the wall are also heated and reach their melting point. From this time onward, the PCMs continue to absorb heat energy from the PV system while resisting an increase in their own temperature. This allows the PCMs to maintain a relatively constant temperature at their melting point, effectively regulating the thermal characteristics. As a result, it is natural that PCM:C18 and PCM:C22 tend to maintain their temperature and the surrounding environment at 302 K and 317 K, respectively, from the beginning to the end of melting. Therefore, reducing the temperature of the PV surface by PCM:C18 and increasing the temperature of the output fluid by PCM:C22 can be justified. Lastly, it should be noted that the above simulations were conducted in about 1 h.

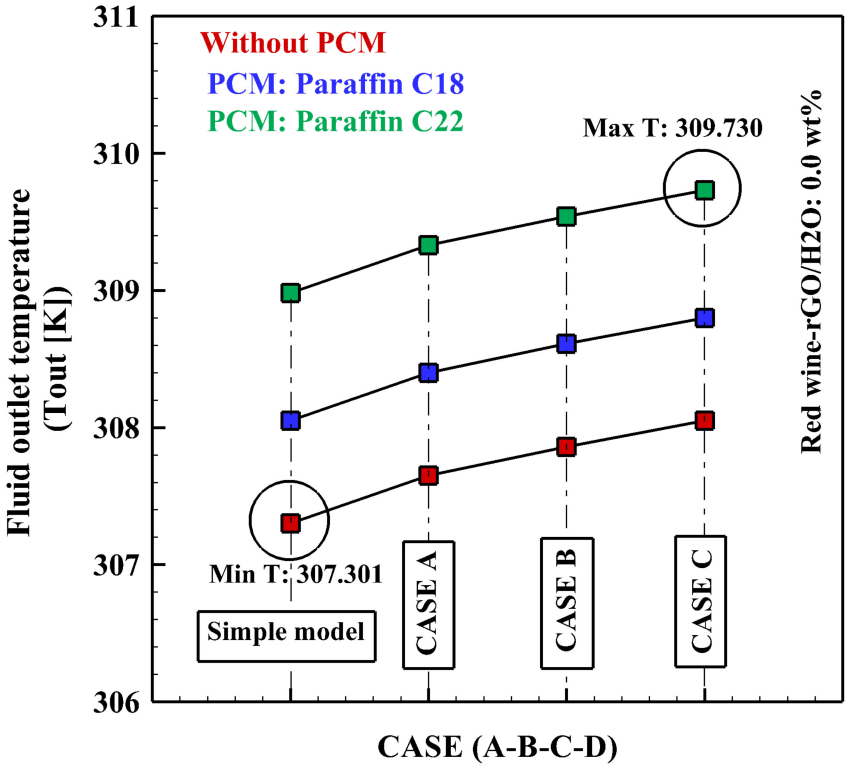

Figure 7. Fluid outlet temperature in different models with and without PCM.

3.2. The Effect of Eco-Friendly Nanofluid on T_{out} and T_{put}

Figure 8a shows the changes in PV cell temperature for different concentrations of red wine-rGO/H_2O nanofluid (ϕ = 1% to 4%) in the presence of PCM:C18, which had the best performance in reducing T_{pvt}. Accordingly, Figure 8b shows the fluid outlet temperature changes for different concentrations of red wine-rGO/H_2O nanofluid (ϕ = 1% to 4%) in the presence of PCM:C22, which had the best performance in increasing Tout. From a physical point of view, adding red wine-rGO nanoparticles to the base fluid (H_2O) changes the flow structure in a manner that not only enhances thermal conductivity but also increases the heat absorption capacity. In fact, various factors such as Brownian diffusion, thermophoresis, dispersion of suspended nanoparticles, irregular movements,

and disturbances of nanoparticles lead to an increase in the energy exchange rate. Consequently, this led to an increase in the temperature gradient between the structure and the fluid. According to Figure 8a, by changing the simulation from W-rGO/H_2O 0.0 wt% to W-rGO/H_2O 4.0 wt% for PV/T with a simple model and PCM:C18, PV cell temperature is reduced by about 0.14%. Physically, after the complete melting of PCMs, their resistance to the increase in temperature of themselves and the surrounding environment will be lost. Therefore, in order to postpone the complete melting of PCMs, nanofluids can be used, which is beneficial for cooling the system. By incorporating the nanofluid within the copper tubes, the phase-change material can be returned to a solid state. This enables the heat exchange process to persist, allowing for the transfer of heat from the module surface to the phase change material and facilitating a change in its state. According to the same argument, by changing the simulation from W-rGO/H_2O 0.0 wt% to W-rGO/H_2O 4.0 wt% for PV/T with a simple model and PCM:C22, the fluid outlet temperature has increased by about 0.1%.

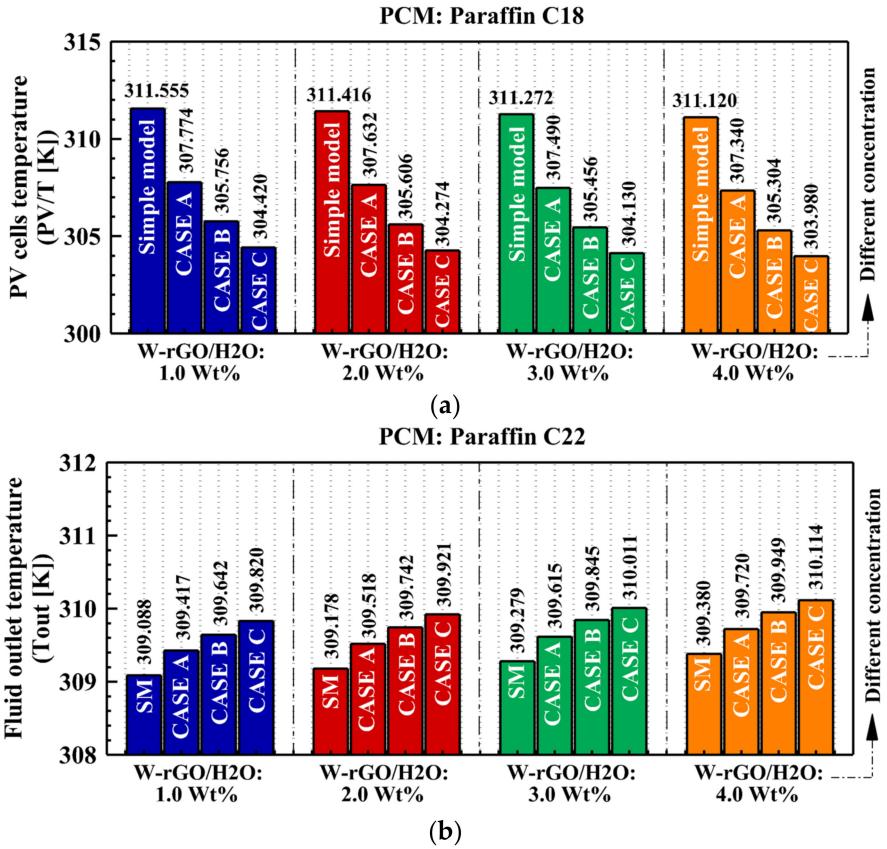

Figure 8. (**a**) PV cell temperature with PCM and different concentrations of nanofluid, and (**b**) fluid outlet temperature with PCM and different concentrations of nanofluid.

3.2.1. Thermal and Electrical Efficiency

The enthalpy of fusion and the fusion temperature are two key factors for PCMs that determine the thermal efficiency and performance improvement of each PCM material [37,38]. Higher outlet fluid temperatures lead to higher thermal efficiency, and lower absorber temperatures lead to higher electrical efficiency. The temperatures of the outlet fluid and the absorber plate using the surface averaging method are presented in Figure 9a,b. It should be noted that due to the higher influence of electrical energy than thermal energy, electrical efficiency plays a greater role in the overall efficiency of PV/T. To investigate the effect of PCM on thermal efficiency, two different PCM models, including PCM:C18 and PCM:C22, were used in three innovative geometries (CASE A–C). The outcomes obtained from these configurations were then compared to the state without PCM, as depicted in Figure 9a. As

observed in Figure 9a, the utilization of paraffin waxes as PCM leads to an enhancement in thermal efficiency. The simulation results demonstrate that when transitioning from the state without PCM to PCM:C18 and PCM:C22 in the PV/T system with a simple model and without the presence of nanofluid, the thermal efficiency has increased by approximately 22.3 and 42.9%, respectively.

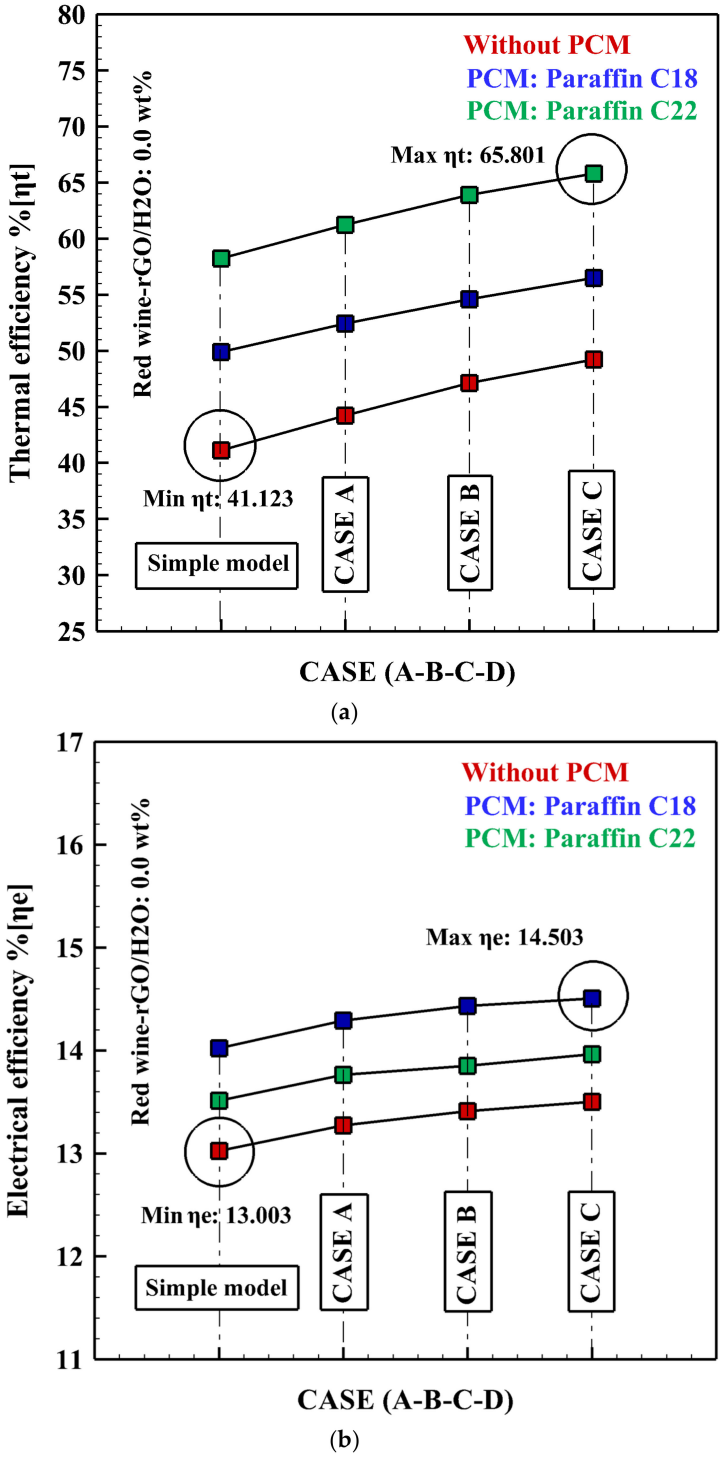

Figure 9. (**a**) Thermal efficiency of PVT systems in different models with PCMs and without PCM, and (**b**) electrical efficiency of PVT systems in different models with PCMs and without PCM.

This phenomenon can be argued based on Equation (8) and the increase in the fluid outlet temperature. It is evident that the geometry of CASE C has more thermal efficiency

than the other two models. This can be attributed to the increased curvature in the flow path (a = 6 and b = 10), which facilitates prolonged fluid residence within the pipe, allowing for a longer duration of heat exchange with the structure. Additionally, paraffin waxes have been able to significantly increase the electrical efficiency of PV. According to Equation (8), the electrical output power is reversely related to the PV cell temperature. The comparison between PCM:C18 and PCM:C22 also shows the superiority of PCM:C18 in increasing electrical efficiency compared to PCM:C22, which originates from the lower absorber temperature in this model of paraffin wax (see Figure 9b).

3.2.2. The Effect of Eco-Friendly Nanofluid on η_{th} and η_{el}

Thermal efficiency is considered one of the important factors in evaluating the performance of thermal photovoltaic collectors. Changes in η_{th} in the presence of PCM:C22 and changes in η_{el} in the presence of PCM:C18 for different concentrations of red wine-rGO/H_2O nanofluid (ϕ = 1% to 4%) are shown in Figure 10a,b, respectively. The increase in the thermal efficiency of the system when using a nanofluid with a higher concentration compared to a nanofluid with a lower concentration is due to the higher thermal conductivity coefficient of nanoparticles. On the other hand, this phenomenon can be argued based on Equation (9) and the increase in the temperature of the outlet fluid due to the Brownian movements of the nanoparticles. Furthermore, the natural tendency of PCM:C18 to maintain its temperature and that of the environment at the melting point (302 K) from the beginning to the end of melting provides the conditions for PCM:C18 to create a lower temperature for the PV cell. With the increase in the concentration of red wine-rGO nanoparticles, the melting time of PCM:C18 is delayed. This delay is beneficial for system cooling since the temperature of PCM starts to rise after complete melting, thereby reducing the temperature gradient between the structure and the fluid. According to the same argument, when changing the simulation from W-rGO/H_2O 0.0 wt% to W-rGO/H_2O 4.0 wt% for PV/T with a simple model and PCM:C18, the electrical efficiency has increased by approximately 0.1%.

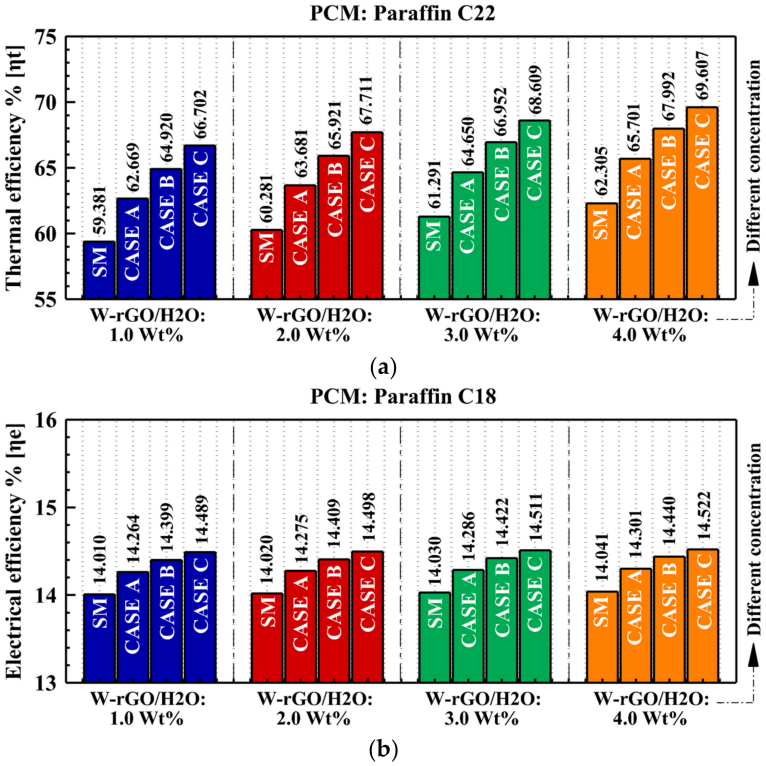

Figure 10. (**a**) Thermal efficiency of PVT systems with PCM and different concentrations of nanofluid; and (**b**) electrical efficiency of PVT systems with PCM and different concentrations of nanofluid.

3.3. The Exergy Analysis

Energy analysis is based on the first law of thermodynamics, and exergy analysis is based on the second law of thermodynamics. Usually, exergy analysis is considered a more appropriate analysis because a difference is made between usable energy and non-usable energy [39,40]. To calculate the exergy terms, the condition of the dead state is assumed, where T_0 = 298 K, P = 100 kP, and the temperature of the sun is 5774 K. Due to the higher quality of electrical energy compared to thermal energy, electrical efficiency plays a greater role in the exergy efficiency of the PV/T system. Consequently, the behavior of exergy efficiency is very similar to the behavior of electrical efficiency. To investigate the effect of PCM on exergy efficiency, two paraffin wax models were used in three innovative geometries (CASE A–C), and the results were compared with the case without PCM (see Figure 11). The results indicate that CASE C exhibits superior exergy efficiency compared to the other two models. This superiority can be attributed to the geometry of CASE C, which achieves both a higher output temperature and a lower PV cell temperature. As a result, according to Equation (10), the exergy efficiency is higher. The comparison between PCM:C18 and PCM:C22 also shows the superiority of PCM:C18 in increasing exergy efficiency compared to PCM:C22. This difference arises from the greater effect of electrical efficiency than thermal efficiency on increasing exergy.

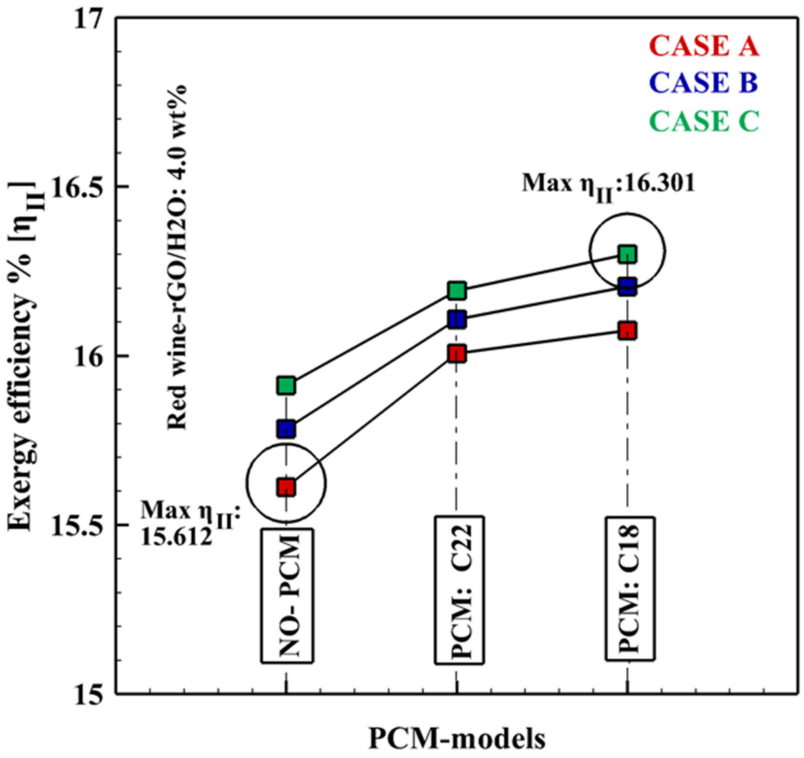

Figure 11. Exergy efficiency of the PVT system in different models with and without PCM.

3.4. The PCM Liquid Fraction

Figure A2 shows the liquid fraction of PCM:C18 on the optimal geometry (CASE C) for different concentrations of red wine-rGO/H_2O nanofluid (ϕ = 1% to 4%). Based on the results, in general, the addition of red wine-rGO nanoparticles increases the heat transfer coefficient of the base fluid (water) compared to the previous state. In fact, the presence of red wine-rGO nanoparticles in turn increases the thermal permeability, which is one of the main reasons for increasing the liquid fraction.

3.5. The PV/T Cell Temperature

Figure 12a shows the effect of three different copper tube models on PVT cell temperature in the presence of 4.0 wt% W-rGO/H_2O nanofluid and without PCMs. It is clear that sinusoidal copper tubes have been more successful in reducing PV cell temperature. Physically, increasing the curvature of the copper tube not only enhances the fluid's heat transfer ability but also prolongs the residence time of the fluid inside the tube. This results in a decrease in PV temperature. Based on these contours, the minimum temperature in the inlet area and the maximum temperature in the air gap area are created. The reason for the increase in temperature in this area is the absence of PCM and cooling fluid tubes. In fact, the air gap has been used as a barrier to prevent heat loss in PV/T systems. The low thermal conductivity of air results in a natural temperature increase within this region. To further investigate CASE C, which has better heat transfer than other models, the temperature contours for two paraffin wax models are displayed (see Figure 12b). A comparison between PCM:C18 and PCM:C22 shows that PCM:C18 produces a more uniform temperature for PV. Physically, after 1 h of simulation, PCM:C18 can better store both sensible heat energy and latent heat energy at the same time.

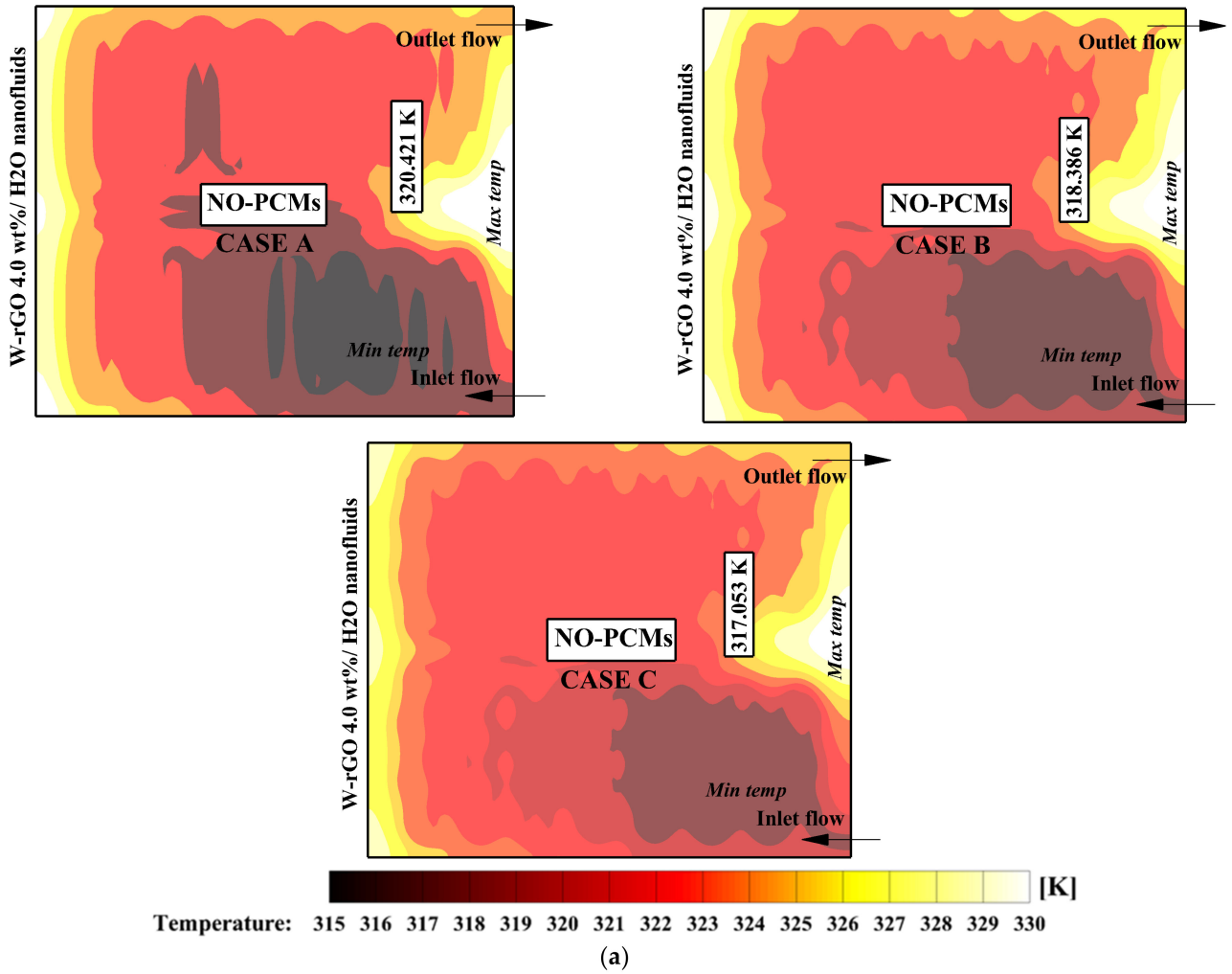

Figure 12. *Cont.*

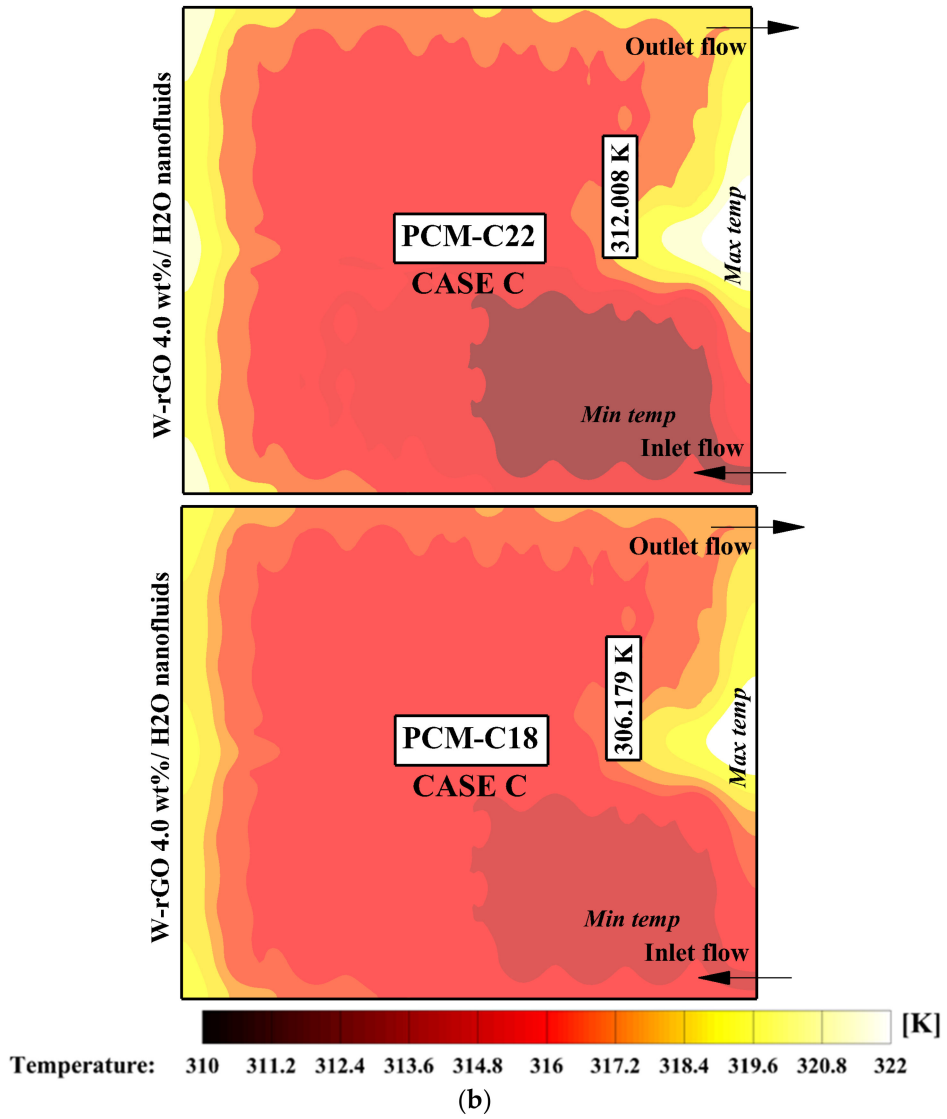

Figure 12. (**a**) PV cell temperature distribution in various models without PCM. (**b**) PV cell temperature distribution in various models with PCM.

4. Conclusions

This study numerically investigated the effect of adding red wine-rGO/H_2O nanofluid to the base fluid as the active coolant and paraffin wax (PCM medium) as the passive coolant of the PVT/PCM system. The effect of the concentration of nanofluid on the enhancement of electrical and thermal efficiency and different parameters of the system were analyzed. The main findings of this study are summarized as follows:

- Using a serpentine tube that creates a more turbulent flow and creates more time for heat transfer (CASE C) is more efficient than other models in all studied items.
- The use of PCM significantly reduces the temperature of the photovoltaic cells. Among the used PCMs, Paraffin C18 has a better performance and reduces the temperature of simple, model A, model B, and model C cells by 4.3, 4.4, 4.7, and 5%, respectively, compared to the model without PCM.
- Paraffin C22 causes the outlet temperature of the fluid to be higher than Paraffin C18 and without PCM. Additionally, by increasing the concentration of nanofluid, the outlet temperature of the fluid can be increased. However, it should be noted that the effect of the concentration of nanofluid on the outlet temperature is insignificant.

- Using model C and paraffin C22 and paraffin C18 causes the thermal and electrical efficiency to increase by 60 and 11.5%, compared to the simple state. The effect of W-rGO/H_2O concentration on thermal efficiency is about 6.33%, and for electrical efficiency, it is about 0.33%.
- The exergy analysis shows that CASE C has more exergy efficiency than the other models due to a higher outlet temperature and a lower cell temperature. Using model C and paraffin 18 increases the exergy efficiency by 4.2% compared to CASE A without PCM.

Author Contributions: H.N.: conceptualization, formal analysis, writing—original draft preparation, visualization. M.G.: software, validation, writing—original draft preparation. M.K.: Methodology, Formal analysis, Writing–review & editing. A.S.: writing—review and editing, supervision, methodology. All authors have read and agreed to the published version of the manuscript.

Funding: This research received no external funding.

Data Availability Statement: The data can be shared up on request.

Conflicts of Interest: The authors declare no conflict of interest.

Appendix A

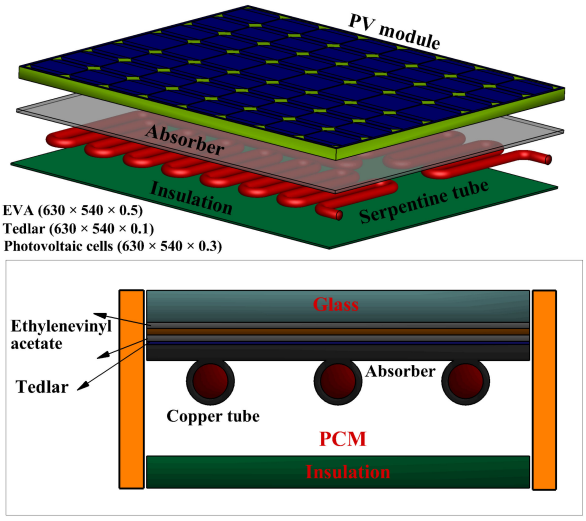

Figure A1. A detailed view of the studied PVT system.

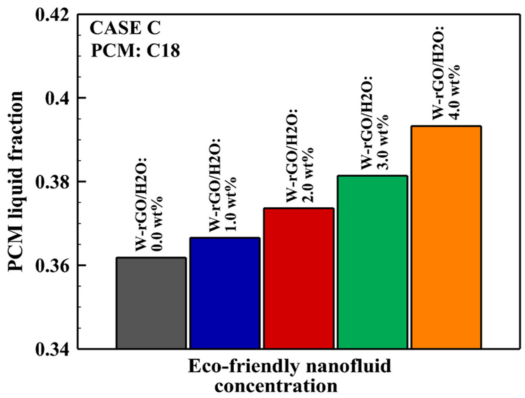

Figure A2. Liquid fraction in CASE C with PCM in various nanofluid mass fractions.

Table A1. Thermal properties of the PVT components.

PV Cells	Copper Collector	TPT	PV Cells	EVA
Type	-	-	Serpentine	Monocrystalline silicone
C_p/J kg^{-1} K^{-1}	385	2090	385	700
Density/kg m^{-3}	8920	960	8920	2330
Thermal conductivity/Wm^{-1} K^{-1}	386.6	0.35	386.6	148

Table A2. UDF codes for the physical properties of the eco-friendly nanofluid.

Physical Properties	Specific Heat Capacity	Thermal Conductivity	Viscosity
W-rGO 1.0 wt%/H_2O nanofluids	C_p = 0.0009 T + 3.8801	k = 0.0004T^2 − 0.0132 T + 0.7089	μ= 0.0002T^2 − 0.0313 T + 1.6015
W-rGO 2.0 wt%/H_2O nanofluids	C_p = 0.0011 T + 3.8251	k = 0.0005T^2 − 0.0158 T + 0.7422	μ= 0.0002T^2 − 0.0327 T + 1.6673
W-rGO 3.0 wt%/H_2O nanofluids	C_p = 0.0016 T + 3.7621	k = 0.0005T^2 − 0.0187 T + 0.7826	μ= 0.0003T^2 − 0.0343 T + 1.7304
W-rGO 4.0 wt%/H_2O nanofluids	C_p = 0.002 T + 3.69640	k = 0.0005T^2 − 0.0193 T + 0.8058	μ= 0.0003T^2 − 0.0349 T + 1.7810

Table A3. The properties of phase change material.

PCM	Heat Capacity (J kg^{-1} K^{-1})	Density (kg m^3)	Melting Temperature (K)	Enthalpy of Fusion (KJ kg^{-1})
Paraffin C22	2950 (l) 2510 (s)	760 (l) 818 (s)	317	226
Paraffin C18	2520	760 (l) 900 (s)	302	244

References

1. Praveenkumar, S.; Agyekum, E.B.; Kumar, A.; Velkin, V.I. Thermo-enviro-economic analysis of solar photovoltaic/thermal system incorporated with u-shaped grid copper pipe, thermal electric generators and nanofluids: An experimental investigation. *J. Energy Storage* **2023**, *60*, 106611. [CrossRef]
2. Hussien, A.; Eltayesh, A.; El-Batsh, H.M. Experimental and numerical investigation for PV cooling by forced convection. *Alex. Eng. J.* **2022**, *64*, 427–440. [CrossRef]
3. Bandaru, S.H.; Becerra, V.; Khanna, S.; Radulovic, J.; Hutchinson, D.; Khusainov, R. A Review of Photovoltaic Thermal (PVT) Technology for Residential Applications: Performance Indicators, Progress, and Opportunities. *Energies* **2021**, *14*, 3853. [CrossRef]
4. Chen, Y.; Guo, M.; Liu, Y.; Wang, D.; Zhuang, Z.; Quan, M. Energy, exergy, and economic analysis of a centralized solar and biogas hybrid heating system for rural areas. *Energy Convers. Manag.* **2023**, *276*, 116591. [CrossRef]
5. Abdul-Ganiyu, S.; Quansah, D.A.; Ramde, E.W.; Seidu, R.; Adaramola, M.S. Techno-economic analysis of solar photovoltaic (PV) and solar photovoltaic thermal (PVT) systems using exergy analysis. *Sustain. Energy Technol. Assess.* **2021**, *47*, 101520. [CrossRef]
6. Nabi, H.; Gholinia, M.; Ganji, D.D. Employing the (SWCNTs-MWCNTs)/H_2O nanofluid and topology structures on the microchannel heatsink for energy storage: A thermal case study. *Case Stud. Therm. Eng.* **2023**, *42*, 102697. [CrossRef]
7. Nazri, N.S.; Fudholi, A.; Mustafa, W.; Yen, C.H.; Mohammad, M.; Ruslan, M.H.; Sopian, M.K. Exergy and improvement potential of hybrid photovoltaic thermal/thermoelectric (PVT/TE) air collector. *Renew. Sustain. Energy Rev.* **2019**, *111*, 132–144. [CrossRef]
8. Ahmadinejad, M.; Moosavi, R. Energy and exergy evaluation of a baffled-nanofluid-based photovoltaic thermal system (PVT). *Int. J. Heat Mass Transf.* **2023**, *203*, 123775. [CrossRef]
9. Dupeyrat, P.; Ménézo, C.; Fortuin, S. Study of the thermal and electrical performances of PVT solar hot water system. *Energy Build.* **2014**, *68*, 751–755. [CrossRef]
10. Alous, S.; Kayfeci, M.; Uysal, A. Experimental investigations of using MWCNTs and graphene nanoplatelets water-based nanofluids as coolants in PVT systems. *Appl. Therm. Eng.* **2019**, *162*, 114265. [CrossRef]
11. Sotehi, O.; Chaker, A.; Maalouf, C. Hybrid PV/T water solar collector for net zero energy building and fresh water production: A theoretical approach. *Desalination* **2016**, *385*, 1–11. [CrossRef]
12. Nasrin, R.; Hasanuzzaman, M.; Rahim, N.A. Effect of high irradiation and cooling on power, energy and performance of a PVT system. *Renew. Energy* **2018**, *116*, 552–569. [CrossRef]
13. Nižetić, S.; Papadopoulos, A.M.; Giama, E. Comprehensive analysis and general economic-environmental evaluation of cooling techniques for photovoltaic panels, Part I: Passive cooling techniques. *Energy Convers. Manag.* **2017**, *149*, 334–354. [CrossRef]
14. Idoko, L.; Anaya-Lara, O.; McDonald, A. Enhancing PV modules efficiency and power output using multi-concept cooling technique. *Energy Rep.* **2018**, *4*, 357–369. [CrossRef]
15. Khodadadi, M.; Sheikholeslami, M. Numerical simulation on the efficiency of PVT system integrated with PCM under the influence of using fins. *Sol. Energy Mater. Sol. Cells* **2021**, *233*, 111402. [CrossRef]

16. Fu, Z.; Li, Y.; Liang, X.; Lou, S.; Qiu, Z.; Cheng, Z.; Zhu, Q. Experimental investigation on the enhanced performance of a solar PVT system using micro-encapsulated PCMs. *Energy* **2021**, *228*, 120509. [CrossRef]
17. Moein-Jahromi, M.; Rahmanian-Koushkaki, H.; Rahmanian, S.; Jahromi, S.P. Evaluation of nanostructured GNP and CuO compositions in PCM-based heat sinks for photovoltaic systems. *J. Energy Storage* **2022**, *53*, 105240. [CrossRef]
18. Javidan, M.; Asgari, M.; Gholinia, M.; Nozari, M.; Asgari, A.; Ganji, D.D. Investigation of convection and radiation heat transfer of paraffinic materials and storage of thermal energy in melting process of PCMs in the cavity with transparent inner walls. *Energy Rep.* **2022**, *8*, 5522–5532. [CrossRef]
19. Alsaiari, A.O.; Shanmugan, S.; Abulkhair, H.; Bamasag, A.; Moustafa, E.B.; Alsulami, R.A.; Ahmad, I.; Elsheikh, A. Applications of TiO2/Jackfruit peel nanocomposites in solar still: Experimental analysis and performance evaluation. *Case Stud. Therm. Eng.* **2022**, *38*, 102292. [CrossRef]
20. Ibrahim, A.M.M.; Omer, M.A.E.; Das, S.R.; Li, W.; Alsoufi, M.S.; Elsheikh, A. Evaluating the effect of minimum quantity lubrication during hard turning of AISI D3 steel using vegetable oil enriched with nano-additives. *Alex. Eng. J.* **2022**, *61*, 10925–10938. [CrossRef]
21. Sardarabadi, M.; Passandideh-Fard, M.; Maghrebi, M.-J.; Ghazikhani, M. Experimental study of using both ZnO/water nanofluid and phase change material (PCM) in photovoltaic thermal systems. *Sol. Energy Mater. Sol. Cells* **2017**, *161*, 62–69. [CrossRef]
22. Nada, S.A.; El-Nagar, D.H.; Hussein, H.M.S. Improving the thermal regulation and efficiency enhancement of PCM-Integrated PV modules using nano particles. *Energy Convers. Manag.* **2018**, *166*, 735–743. [CrossRef]
23. Ghadikolaei, S.S.; Siahchehrehghadikolaei, S.; Gholinia, M.; Rahimi, M. A CFD modeling of heat transfer between CGNPs/H2O Eco-friendly nanofluid and the novel nature-based designs heat sink: Hybrid passive techniques for CPU cooling. *Therm. Sci. Eng. Prog.* **2023**, *37*, 101604. [CrossRef]
24. Siahchehrehghadikolaei, S.; Gholinia, M.; Ghadikolaei, S.S.; Lin, C.-X. A CFD modeling of CPU cooling by eco-friendly nanofluid and fin heat sink passive cooling techniques. *Adv. Powder Technol.* **2023**, *33*, 103813. [CrossRef]
25. Cui, Y.; Zhu, J.; Zhang, F.; Shao, Y.; Xue, Y. Current status and future development of hybrid PV/T system with PCM module: 4E (energy, exergy, economic and environmental) assessments. *Renew. Sustain. Energy Rev.* **2022**, *158*, 112147. [CrossRef]
26. Al-Musawi, A.I.A.; Taheri, A.; Farzanehnia, A.; Sardarabadi, M.; Passandideh-Fard, M. Numerical study of the effects of nanofluids and phase-change materials in photovoltaic thermal (PVT) systems. *J. Therm. Anal. Calorim.* **2019**, *137*, 623–636. [CrossRef]
27. Al-Abidi, A.A.; Mat, S.; Sopian, K.; Sulaiman, M.Y.; Mohammad, A.T. Numerical study of PCM solidification in a triplex tube heat exchanger with internal and external fins. *Int. J. Heat Mass Transf.* **2013**, *61*, 684–695. [CrossRef]
28. Ehms, J.N.; Oliveski, R.D.C.; Rocha, L.O.; Biserni, C. Theoretical and numerical analysis on phase change materials (PCM): A case study of the solidification process of erythritol in spheres. *Int. J. Heat Mass Transf.* **2018**, *119*, 523–532. [CrossRef]
29. Evans, D.L. Simplified method for predicting photovoltaic array output. *Sol. Energy* **1981**, *27*, 555–560. [CrossRef]
30. Sardarabadi, M.; Passandideh-Fard, M.; Heris, S.Z. Experimental investigation of the effects of silica/water nanofluid on PV/T (photovoltaic thermal units). *Energy* **2014**, *66*, 264–272. [CrossRef]
31. Nabi, H.; Pourfallah, M.; Gholinia, M.; Jahanian, O. Increasing heat transfer in flat plate solar collectors using various forms of turbulence-inducing elements and CNTs-CuO hybrid nanofluids. *Case Stud. Therm. Eng.* **2022**, *33*, 101909. [CrossRef]
32. Saidur, R.; BoroumandJazi, G.; Mekhlif, S.; Jameel, M. Exergy analysis of solar energy applications. *Renew. Sustain. Energy Rev.* **2012**, *16*, 350–356. [CrossRef]
33. Sadri, R.; Hosseini, M.; Kazi, S.; Bagheri, S.; Zubir, N.; Ahmadi, G.; Dahari, M.; Zaharinie, T. A novel, eco-friendly technique for covalent functionalization of graphene nanoplatelets and the potential of their nanofluids for heat transfer applications. *Chem. Phys. Lett.* **2017**, *675*, 92–97. [CrossRef]
34. Sadri, R.; Hosseini, M.; Kazi, S.; Bagheri, S.; Zubir, N.; Solangi, K.; Zaharinie, T.; Badarudin, A. A bio-based, facile approach for the preparation of covalently functionalized carbon nanotubes aqueous suspensions and their potential as heat transfer fluids. *J. Colloid Interface Sci.* **2017**, *504*, 115–123. [CrossRef] [PubMed]
35. Zhang, C.; Ping, J.; Ying, Y. Evaluation of trans-resveratrol level in grape wine using laser-induced porous graphene-based electrochemical sensor. *Sci. Total. Environ.* **2020**, *714*, 136687. [CrossRef] [PubMed]
36. Shahsavar, A.; Eisapour, M.; Talebizadehsardari, P. Experimental evaluation of novel photovoltaic/thermal systems using serpentine cooling tubes with different cross-sections of circular, triangular and rectangular. *Energy* **2020**, *208*, 118409. [CrossRef]
37. Mousavi, S.; Kasaeian, A.; Shafii, M.B.; Jahangir, M.H. Numerical investigation of the effects of a copper foam filled with phase change materials in a water-cooled photovoltaic/thermal system. *Energy Convers. Manag.* **2018**, *163*, 187–195. [CrossRef]
38. Morad, A.M.; Selima, E.S.; Abu-Nab, A.K. Thermophysical bubble dynamics in N-dimensional Al2O3/H2O nanofluid between two-phase turbulent flow. *Case Stud. Therm. Eng.* **2021**, *28*, 101527. [CrossRef]

39. Abu-Nab, A.K.; Selima, E.S.; Morad, A.M. Theoretical investigation of a single vapor bubble during Al_2O_3/H_2O nanofluids in power-law fluid affected by a variable surface tension. *Phys. Scr.* **2021**, *96*, 035222. [CrossRef]
40. Abu-Nab, A.K.; Morad, A.M.; Selima, E.S. Impact of magnetic-field on the dynamic of gas bubbles in N-dimensions of non-Newtonian hybrid nanofluid: Analytical study. *Phys. Scr.* **2022**, *97*, 105202. [CrossRef]

Disclaimer/Publisher's Note: The statements, opinions and data contained in all publications are solely those of the individual author(s) and contributor(s) and not of MDPI and/or the editor(s). MDPI and/or the editor(s) disclaim responsibility for any injury to people or property resulting from any ideas, methods, instructions or products referred to in the content.